Available online at www.sciencedirect.com
ScienceDirect
Journal of Nuclear Materials 361 (2007) 30–40
journal of nuclear materials
www.elsevier.com/locate/jnucmat

Steam oxidation of Zr–1.5Nb–0.4Sn–0.2Fe–0.1Cr and Zircaloy-4 at 900–1200 °C

Jong Hyuk Baek *, Yong Hwan Jeong

Advanced Core Materials Lab., Korea Atomic Energy Research Institute, P.O. Box 105, Yuseong, Daejeon 305-600, South Korea

Received 24 February 2006; accepted 13 October 2006

Abstract

The steam oxidation characteristics for the Zr–1.5Nb–0.4Sn–0.2Fe–0.1Cr (HANA-4) and Zircaloy-4 claddings were elucidated at LOCA temperatures of 900–1200 °C by using a modified thermo-gravimetric analyzer. After the oxidation tests, the oxidation behaviors, oxidation rates, surface appearances, and microstructures of the as-received, as-oxidized, and burn-up simulated claddings were evaluated in this study. The high-temperature oxidation resistance of the as-received HANA-4 cladding was superior to that of the Zircaloy-4. The superior oxidation resistance of the HANA-4 cladding could be attributed to the higher Nb and the lower Sn within its cladding. The pre-oxidized layer formed at the low temperatures below 500 °C could retard the oxidation rate at the high temperatures above 900 °C. And the soundness of the pre-oxidized layer formed at a lower temperature could influence the oxidation kinetics and the rate constants during a steam oxidation at LOCA temperatures from 900 to 1200 °C.

PACS: 42.81.B; 81.65.M; 81.65.K

1. Introduction

In a light water reactor, the fuel cladding plays an important role of preventing leakage of radioactive materials into the coolant as well as transferring the heat generated in the fuel into the coolant [1]. So, the mechanical integrity of the cladding should be guaranteed under the conditions of normal and transient operation, including the design based severe accidents such as a loss of coolant accident (LOCA) and reactivity initiated accident (RIA). During a typical LOCA condition, the cladding is subjected to a high-temperature oxidation which is finally quenched because of an emergency coolant reflooding into the core. In this situation, the current LOCA criteria consist of five separate limits or requirements: (1) peak cladding temperature, (2) maximum cladding oxidation, (3) maximum hydrogen generation, (4) coolable geometry, and (5) long-term cooling [2]. On concerning the high-temperature oxidation of cladding, the equivalent cladding reacted (ECR) should not exceed the criterion of 17% and the peak cladding temperature (PCT) should also be below 1200 °C.

The current trend for nuclear fuel is to increase the fuel discharge burn-up and its cycle length

* Corresponding author. Tel.: +82 42 868 8823; fax: +82 42 862 0432.
E-mail address: jhbaek@kaeri.re.kr (J.H. Baek).

0022-3115/$ - see front matter © 2006 Elsevier B.V. All rights reserved.
doi:10.1016/j.jnucmat.2006.10.015

because of the major advantages in its fuel cycle cost and spent fuel management. At a high burn-up, fuel rods fabricated from conventional Zircaloys often exhibit a significant degradation such as an oxidation, hydriding and oxide spallation. Many fuel vendors have developed advanced claddings, such as ZIRLO, M5, MDA, and NDA, for the high burn-up fuel to improve their safety and economical efficiency [3–7]. Korea is also developing advanced claddings for a high burn-up fuel above 70 GWD/tU [8,9]. The composition of the Korean advanced claddings, which were named HANA claddings, consisted of Zr, Nb, Sn, Fe, Cr, and Cu. The chemical compositions of the HANA claddings are different from those of the conventional Zircaloys. Particularly, Nb is added in the range of 0.4–1.5 wt% as one of the major alloying elements. Because of the different composition of the HANA claddings in comparison with the conventional Zircaloy-4, their integrity of the HANA claddings under the LOCA condition should be evaluated.

Most studies have been focused on the steam oxidation of the as-received cladding state [10–16], because the steam oxidation of the cladding during a LOCA occurs at high temperatures above 800 °C. Practically, however, since a LOCA occurs suddenly during the normal operation of a nuclear power plant, the fuel cladding, which has been oxidized on the outer surface and hydrided in the matrix during the operation period, would undergo a LOCA experience. Although some researches have reported on the effects of a pre-oxidization and a pre-hydrogenation in the Zircaloy claddings on a steam oxidation at LOCA temperatures [17,18], a detailed understanding of the effects has not be found as yet. As these researches were confined to Zircaloy claddings, it is necessary to expand the research on the effects to advanced Nb-containing Zr claddings. In this study, the steam oxidation characteristics of two claddings (HANA-4 and Zircaloy-4) were systematically elucidated from the viewpoints of the oxidation behaviors, oxidation rates, surface appearances, and microstructures of the as-received, pre-oxidized, and pre-hydrogenated/pre-oxidized claddings.

2. Experimental

The chemical composition of the two claddings used in this study is shown in Table 1. During a steam oxidation testing, the samples consisted of three kinds of specimens with the following conditions: (1) as-received, (2) pre-oxidized, and (3) pre-hydrogenated/pre-oxidized. For case (1), the specimens (~7 wppm H) were prepared by cutting ring-like specimens of 8 mm in length. Both ends of the specimens were ground carefully up to Grit No. 1200 of SiC paper. Then all the specimens were pickled in a solution of 5% HF, 45% HNO_3, and 50% H_2O. For case (2), the pre-oxide layer on the surface was formed by corroding it in a static autoclave with 450 °C pure steam (10.3 MPa). The oxide thicknesses were estimated by a calculation of the periodical measurements of the weight gain and they were nearly 6 μm for all the specimens. For case (3), the charging hydrogen contents and the forming oxide thickness were determined, with the intention of simulating the irradiated Zircaloy-4 claddings in a PWR [19]. The 30 μm oxide specimens with 250 wppm H and the 80 μm ones with 250 wppm H were prepared by hydrogenating them gaseously at 400 °C and then oxidizing them at 500 °C in air. All the prepared specimens were analyzed for hydrogen using the hot vacuum extraction mass spectrometry (HVEMS) technique.

Table 1
Chemical composition of the Zr claddings

Claddings	Nb (wt%)	Sn (wt%)	Fe (wt%)	Cr (wt%)	Zr (wt%)
HANA-4	1.5	0.4	0.2	0.1	Bal.
Zircaloy-4	–	1.38	0.2	0.1	Bal.

The apparatus for the high-temperature testing was established by modifying the Shimadzu TGA (thermo-gravimetric analyzer, TGA 51H), as described in a previous study [20]. The specimens were hung on a microbalance above an electric furnace. The balance chamber was purged with a argon backflow to prevent the ingress of steam. A steam generator was attached to the apparatus to supply steam continuously into the furnace. Steam flow was maintained at a constant rate during the oxidation test. The steam supply rate was 0.6 g/cm^2 min (STP) at 1 atm. This steam flow rate was adequate enough to satisfy the conditions for a high-temperature oxidation between the steam and the Zr claddings without a steam starvation on the basis of a review of previous literatures [21,22]. The weight change was measured by an in situ method to within ±0.001 mg during the oxidation reaction. The distance between the specimen and the thermocouple

junctions was about 2 mm. Because this separation could introduce temperature measurement errors, preliminary tests were performed by comparing thermocouple reading to another one which was attached directly to the specimen. The difference between the temperature reading from the thermocouple in the furnace and the one attached to the specimen was less than 5 °C in the temperature ranges of 900–1200 °C. In flowing steam, the temperature became a maximum but returned to the desired value in less than 20 s. In order to prevent the specimen from oxidizing during the heat-up to the desired temperature, high purity (99.999%) Ar gas was purged into the furnace thus not affecting the weighing accuracy of the electric balance. The heat-up rate to the desired temperature was set at 50 °C/min. The prepared steam was supplied into the furnace right after the temperature reached the desired level. After an oxidation testing at the LOCA temperatures of 900–1200 °C for 2400 s, the surface appearances and microstructures of the oxidized specimens were carefully observed by a close-focused camera and an optical microscope.

3. Results and discussion

3.1. As-received claddings

When the steam oxidation tests of the Zr claddings were carried out by using a TGA, the weight gains were directly detected from the reaction between the Zr and the steam. The weight gains were deduced from the amount of absorbed oxygen ($W_{\text{oxygen absorbed}}$) during the oxidation reaction.

The weight gains of HANA-4 from the steam oxidization test performed at 900–1200 °C for up to 2400 s are presented in Fig. 1, and compared with those of Zircaloy-4. The weight gains of both Zr claddings increased with an increase of the oxidation time. The weight gains of the HANA-4 claddings were lower than those of the Zircaloy-4 at the same oxidation temperature. It is thought that the oxidation resistance improvement of HANA-4 could have resulted from a difference in the alloying composition. It was anticipated that the Nb as well as Sn within the HANA-4 cladding could have improved its oxidation resistance at high temperatures above 900 °C. The oxidation kinetics of both

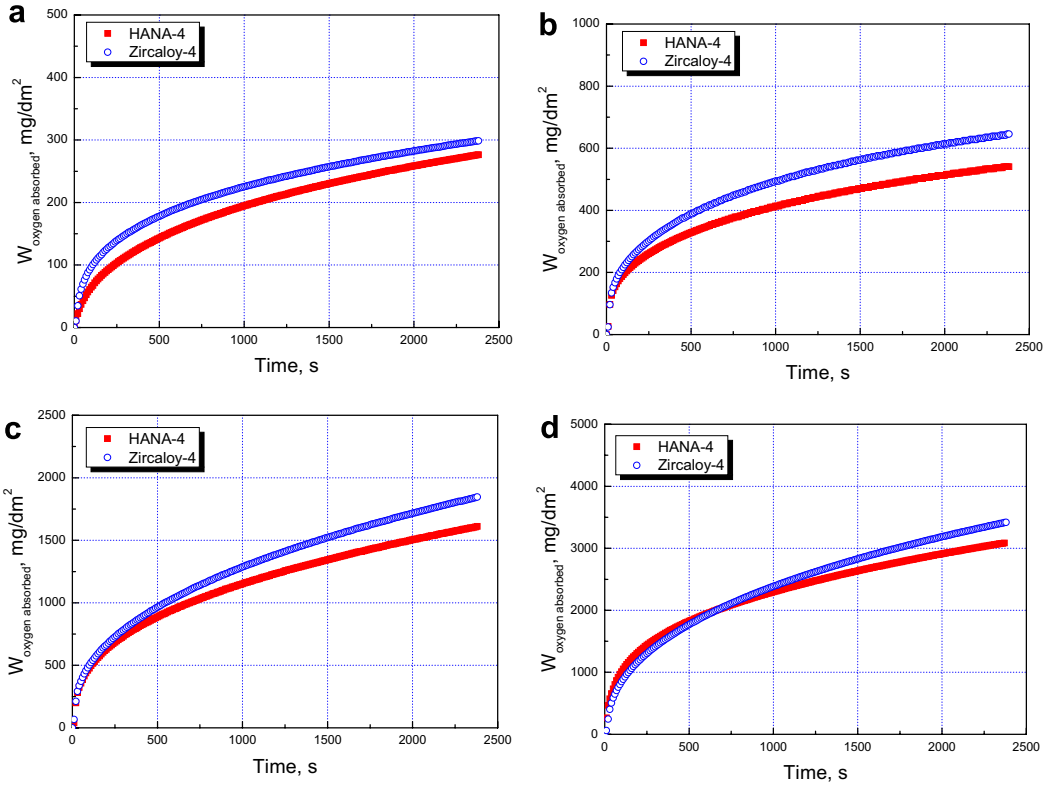

Fig. 1. Oxidation behaviors of the as-received Zr claddings: (a) 900 °C, (b) 1000 °C, (c) 1100 °C and (d) 1200 °C.

claddings at the early stages obeyed the parabolic rate law. The obedience for the parabolic rate law increased as the oxidation temperature increased. This is the reason why the oxidation reaction would be more active at higher temperature.

In general, because the oxidation rate at LOCA temperatures above 900 °C could be strongly dependent upon the test temperature and time during the oxidation reaction, the weight gains at the early stages could have resulted from an oxygen diffusion through the oxide layer in accordance with the parabolic rate [18,23]. The relationship between the weight gain and the exposure time is as follows:

$$(W_{\text{oxygen absorbed}})^2 = K_p \cdot t, \quad (1)$$

where, $W_{\text{oxygen absorbed}}$ denotes the weight gain (mg/dm^2) of the absorbed oxygen by the oxidation reaction, K_p the parabolic rate constant (mg^2/dm^4 s), and t the exposure time (s).

The parabolic rate constant (K_p) during the oxidation was strongly dependent on the temperature. So,

$$K_p = A \cdot \exp(-Q/RT), \quad (2)$$

where, A is a constant (mg^2/dm^4 s), Q the activation energy for the oxidation reaction, R a universal gas constant (8.314 J/mol K), and T the oxidation temperature (K).

The parabolic rate constants of both as-received HANA-4 and Zircaloy-4 claddings were analyzed by Eqs. (1) and (2), and the results are shown in Fig. 2. The oxidation rate constants of the HANA-4 claddings were lower than those of the Zircaloy-4. There was little difference in the rate constants at 1200 °C. But, as the oxidation temperature decreased, the rate constants for both claddings decreased.

Although the difference of the oxidation rate constants in comparison with results from the present study and the Pawel et al. [24] might be of a complex nature, e.g. caused by different steam-flow carrier gas or different steam flow direction, it could be possible to compare with the both results because of the same method in the weight gain measurement for the evaluation of the oxygen uptakes. In Fig. 2, the rate constants by the Cathcart–Pawel correlation [24] are also represented to compare them with those of the present claddings. The rate constants of HANA-4 and Zircaloy-4 in this study were in the lower region when compared with the Cathcart–Pawel ones. In the case of the Zircaloy-4 cladding, there was a large difference in the oxidation rate

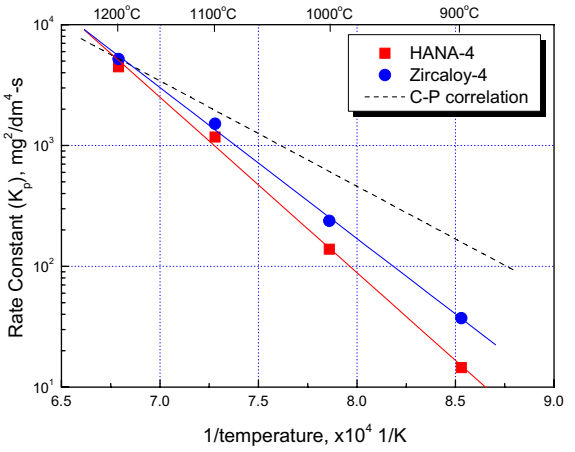

Fig. 2. Rate constants of the as-received Zr claddings.

constants between the present data and the Cathcart–Pawel ones. This could have been caused by the different experimental methods and the temperature ranges. The absorbed oxygen was directly determined by the weight gain method by using a TGA in the present study. Meanwhile, in the Cathcart–Pawel study, the oxygen consumption was calculated from the oxide thickness and the α-Zr layer thickness by the metallographic method. It was noted that the absorbed oxygen level could be underestimated in the Cathcart–Pawel study. Besides, because the oxidation temperatures in the Cathcart–Pawel study ranged from 900 to 1500 °C, there was some inconstancy in the lower temperature ranges at less than 1000 °C, at which the absorbed oxygen level was relatively small. Compared with the Cathcart–Pawel correlation, the oxidation experimental results obtained from the present study were more conservative below 1000 °C than those from the correlation on the basis of the lower rate constants of the HANA-4 cladding.

3.2. Pre-oxidized claddings

Before the steam oxidation, all the specimens had nearly the same oxide thickness (~6 μm), because they were simultaneously pre-oxidized in 450 °C steam. Fig. 3 shows the oxidation behaviors of the pre-oxidized Zr claddings. From Figs. 1 and 3, the weight gains of the pre-oxidized claddings were lower when compared with those of the as-received ones. It was concluded that the pre-oxide layer could affect the oxidation reaction at the LOCA

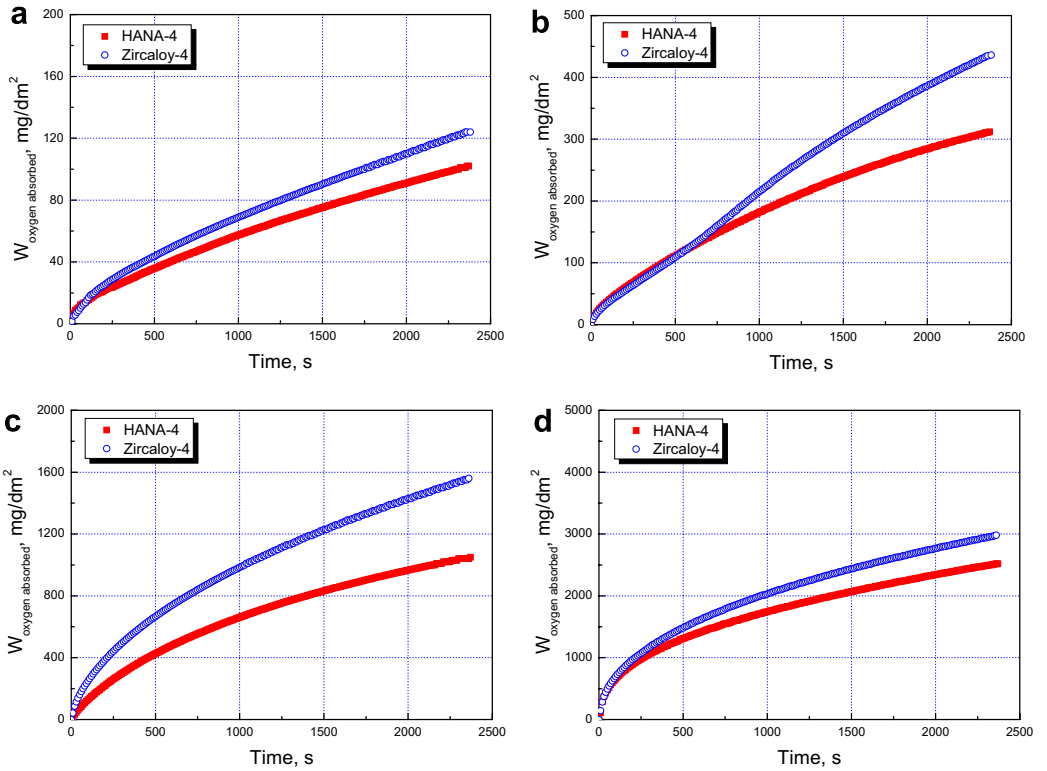

Fig. 3. Oxidation behaviors of the pre-oxidized Zr claddings: (a) 900 °C, (b) 1000 °C, (c) 1100 °C and (d) 1200 °C.

temperatures. And, the weight gains of the pre-oxidized HANA-4 cladding were lower than those of the pre-oxidized Zircaloy-4 at all the oxidation temperatures. This means that the oxidation resistance of the pre-oxidized HANA-4 cladding was superior to that of the pre-oxidized Zircaloy-4. This could have resulted from the different compositions of the two claddings, as previously mentioned. It was found that the oxidation kinetics of the pre-oxidized claddings followed the parabolic rate law similar to the as-received HANA-4. But, the oxidation behavior of the pre-oxidized Zircaloy-4 cladding at 1000 °C showed a rate transition after 700 s. In the case of the pre-oxidized Zircaloy-4 at 1000 °C, the rate constants were calculated from the weight gain data before 700 s. It is not clear why the rate transition occurred at 1000 °C. Probably, it could be related to the phase transformation of the oxide crystal structure [18].

Fig. 4 shows the oxidation rate constants of both the pre-oxidized claddings together with those of the as-received claddings. In the case of the pre-oxidized claddings, the rate constants of HANA-4 were also lower than those of Zircaloy-4. This was the same

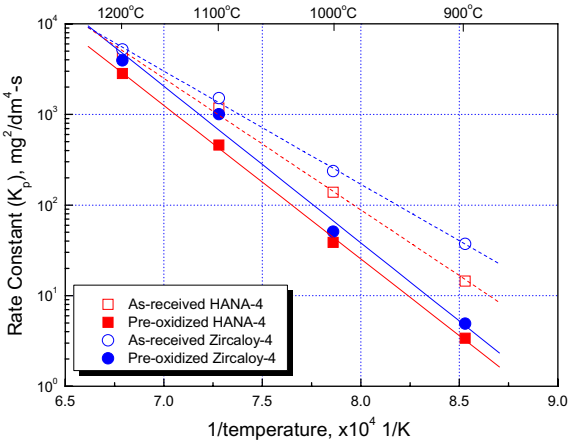

Fig. 4. Rate constants of the pre-oxidized Zr claddings.

trend as the as-received claddings, as discussed in Fig. 2. The Nb addition to the HANA-4 cladding could improve the high-temperature oxidation resistance at temperatures of 900–1200 °C. It is thought that the oxide protectiveness is improved by a niobium addition in Zr alloys. It can be interpreted that

an oxygen diffusion would be retarded during a steam oxidation due to a Nb addition in Zr alloys.

The rate constants of both the pre-oxidized claddings were lower than those of the as-received claddings at all the oxidation temperatures. This present study clearly shows that the oxidation resistance of the pre-oxidized claddings was improved by the pre-oxide layer. But the pre-oxidizing effects on the oxidation resistance were reduced as the oxidation temperatures increased. The retardation effect of the pre-oxidization on a high-temperature oxidation has been published previously by several researches [17,25–27]. They also pointed out that the oxidation suppression effects by the pre-formed oxide were more apparent at higher temperatures. From their results, the exact reason for this phenomenon has not been sufficiently clarified as yet. But one assumption has been considered by the physical property difference of the oxides between that formed at a low temperature of around 450 °C and that formed at a high temperature above 900 °C. At a higher temperature of 1100 or 1200 °C, especially, a diffusion of the oxygen in the pre-oxidized layer might be faster than that in the oxide layer formed at relatively lower temperatures of 900 and 1000 °C. The oxide morphologies at 1100 or 1200 °C were also transformed into more columnar structures, in which the oxygen diffusion along the oxide grain boundary was easier than the oxide morphologies formed at 900 or 1000 °C. So, the pre-oxidization effects had almost disappeared at the higher temperatures of 1100 and 1200 °C. But at relatively lower oxidation temperatures of 900 and 1000 °C, the oxygen diffusion rate in the pre-oxidized layer might decrease to a value equivalent to that in the oxide layer formed in those temperature ranges. Thus this could lead to the suppression of an oxidation at 900 and 1000 °C due to the pre-oxidized layer formed at 450 °C.

3.3. Pre-hydrogenated/pre-oxidized claddings

As mentioned previously, the effects of a pre-oxidization on a steam oxidation at the LOCA temperatures are not fully understood as yet. Furthermore, the effects of a burn-up extension on a high-temperature oxidation above 900 °C, namely the effects of the existence of an oxide layer on the cladding

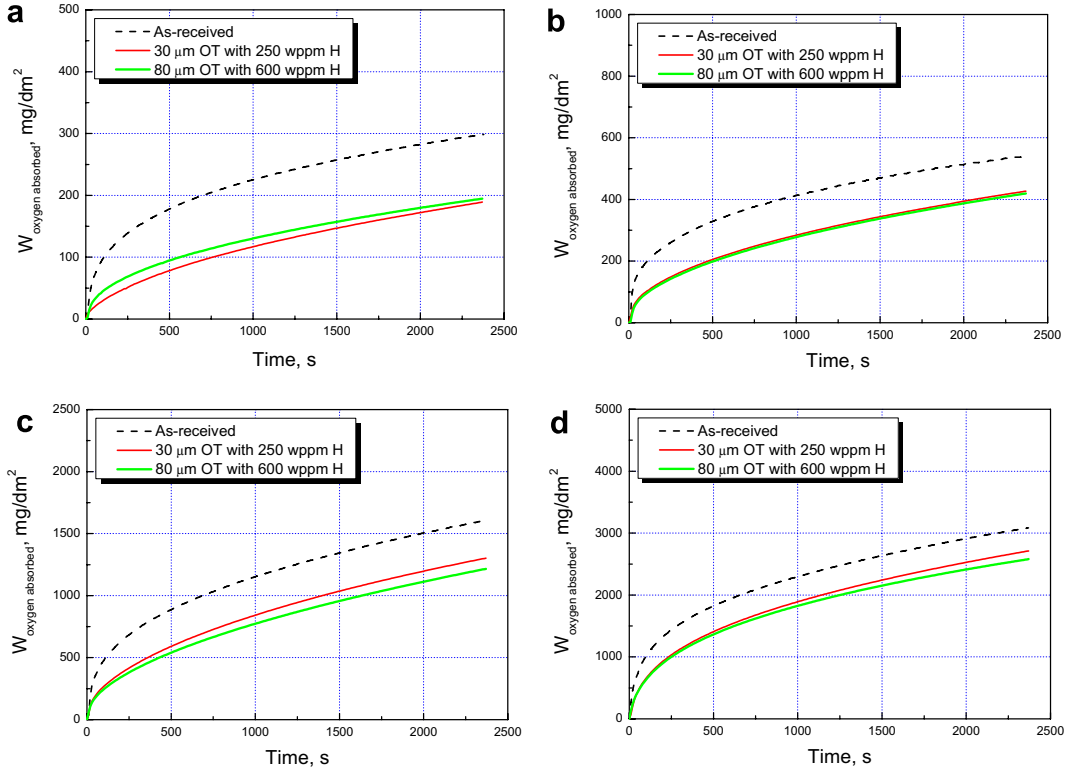

Fig. 5. Oxidation behaviors of the pre-hydrogenated/pre-oxidized HANA-4 claddings: (a) 900 °C, (b) 1000 °C, (c) 1100 °C and (d) 1200 °C.

surface and the hydrogen absorption during a normal operation, are not sufficiently understood and the number of researches is limited [25,26]. Figs. 5 and 6 show the oxidation behaviors of the pre-hydrogenated and the pre-oxidized HANA-4 and Zircaloy-4 claddings, respectively. In the case of the HANA-4 claddings as shown in Fig. 5, the weight gains of the pre-hydrogenated/pre-oxidized claddings were lower than those of the as-received claddings. The retardation effects of the pre-oxidized layer were revealed in the pre-hydrogenated/pre-oxidized claddings of HANA-4. But, the difference in the weight gains between the two pre-hydrogenated/pre-oxidized claddings having 30 μm oxide-thickness (OT) with 250 wppm H and 80 μm OT with 600 wppm was so small that it was regarded as negligible. At all the test temperatures, the oxidation kinetics of the pre-hydrogenated/pre-oxidized claddings was controlled by the parabolic rate law.

The weight gains of the pre-hydrogenated/pre-oxidized Zircaloy-4 claddings were also found in the lower region when compared with those of the as-received ones, as shown in Fig. 6. These are the same trends as the HANA-4 claddings. In the case of the pre-hydrogenated/pre-oxidized Zircaloy-4 claddings, however, the weight gains of the samples having 80 μm OT with 600 wppm H were higher than those of the 30 μm OT with 250 wppm H. It is thought that this could have been caused by the vertical cracks within the pre-oxide layer formed during the specimen preparation process. Fig. 7 shows several vertical cracks within the oxide layer, which were examined after the preparation of the Zircaloy-4 samples having 80 μm OT with 600 wppm H. But they were not detected in other samples such as the 30 μm OT with 250 wppm H and the 80 μm OT with 600 wppm H of the HANA-4 claddings as well as the 30 μm OT with 250 wppm H of the Zircaloy-4 claddings. It is anticipated that the crack existence within the oxide layer in the Zircaloy-4 claddings having 80 μm OT with 600 wppm H could be caused by a lower oxidation resistance of the cladding during the preparation process at 500 °C. In other words, since the oxidation resistance of the HANA-4 cladding was better than that of the Zircaloy-4 at that temperature, vertical cracks would not develop within the oxide layer of HANA-4 in spite of the same preparation

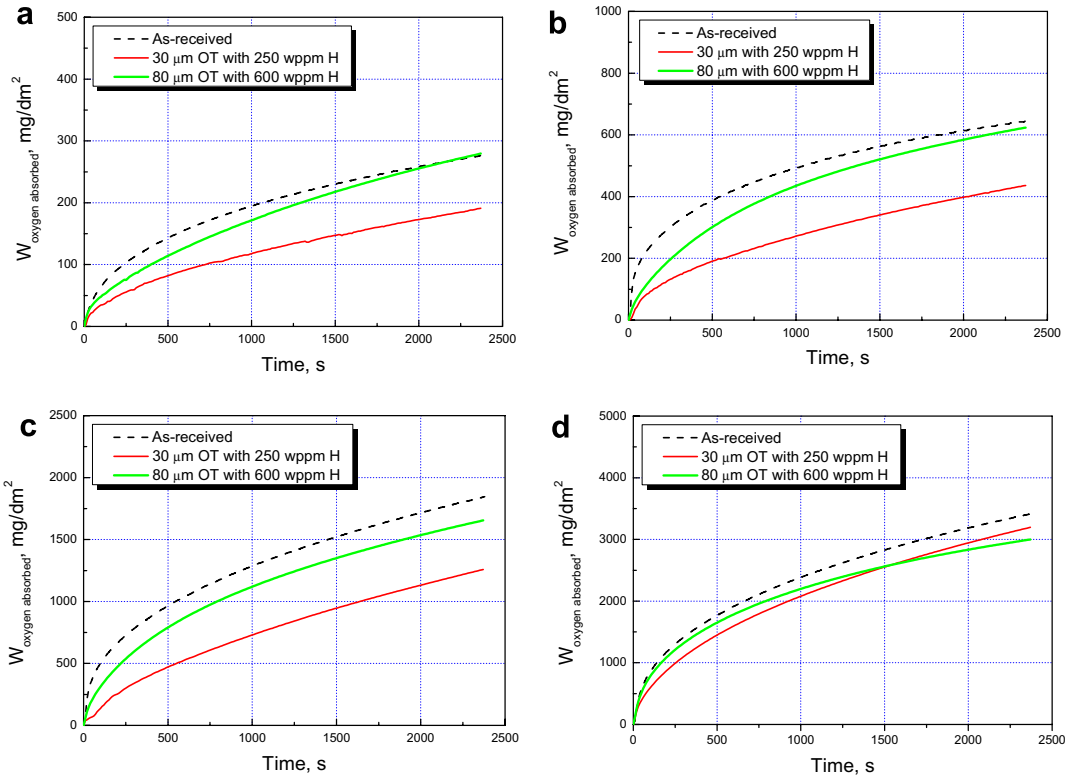

Fig. 6. Oxidation behaviors of the pre-hydrogenated/pre-oxidized Zircaloy-4 claddings: (a) 900 °C, (b) 1000 °C, (c) 1100 °C and (d) 1200 °C.

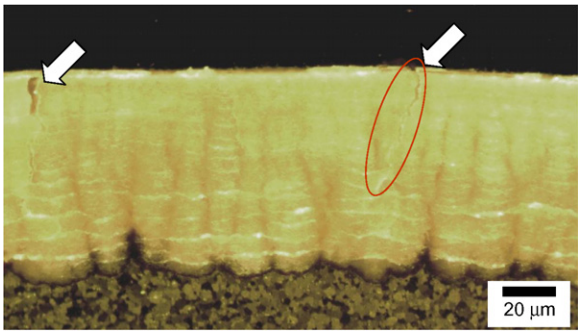

Fig. 7. Vertical cracks within the oxide layer in the Zircaloy-4 samples having 80 μm OT with 600 wppm H.

condition. Coming back to Fig. 6, thus the existing vertical cracks would accelerate the steam oxidation reaction at high temperatures above 900 °C. But, since the oxygen diffusion was rapid in the pre-formed oxide layer at 1200 °C, an accelerated oxidation due to the vertical cracks disappeared. A pre-hydrogenation (up to 740 wppm) of the Zr claddings is known not to influence a steam oxidation at the LOCA temperatures on the basis of previous studies [17,26]. In the present study, the hydrogenation effects on a steam oxidation were considered not to have occurred significantly in the HANA-4 and Zircaloy-4 claddings and they are thus not included in the discussion parts.

The oxidation rates of the pre-hydrogenated/pre-oxidized HANA-4 and Zircaloy-4 claddings were also represented by the parabolic rate law. The oxidation rate constants for all the experimental variations were obtained from the oxidation rate at each oxidation temperature. Fig. 8 shows the oxidation rate constants of the pre-hydrogenated/pre-oxidized HANA-4 and Zircaloy-4 claddings, respectively, including the pre-oxidized and the as-received claddings. In Fig. 8(a), the oxidation rate constants of both the pre-hydrogenated/pre-oxidized HANA-4 claddings were lower than those of the as-received ones. As noted in the oxidation behaviors of Fig. 5, there was little difference in the rate constants of the pre-hydrogenated/pre-oxidized HANA-4 claddings. This means that the effects of a pre-oxidized layer of more than 30 μm in oxide thickness could almost be the same as long as the vertical cracks do not exist within the oxide layer. And, it is also possible to compare the rate constants of the pre-hydrogenated/pre-oxidized HANA-4 claddings with those of the pre-oxidized ones. The oxidation rate constants of the pre-oxidized claddings

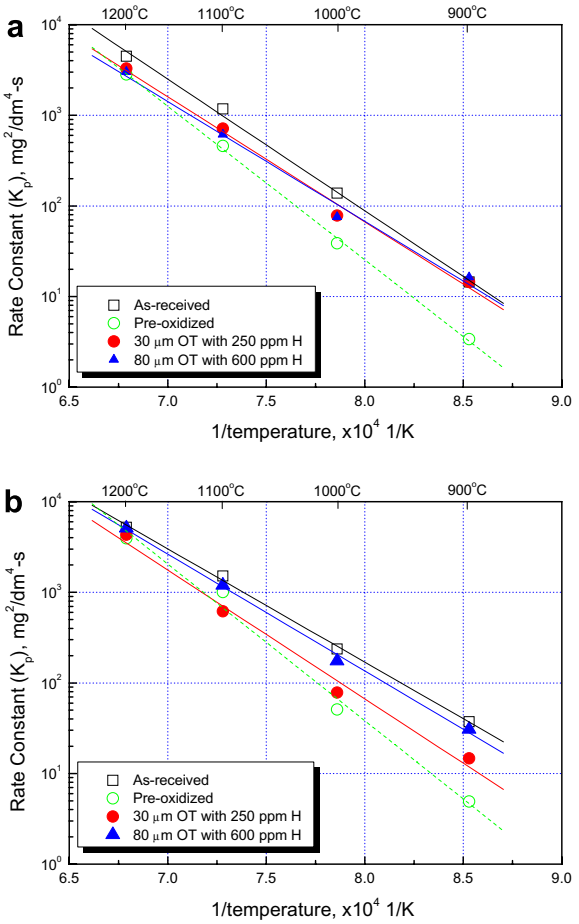

Fig. 8. Rate constants of the Zr claddings: (a) HANA-4, (b) Zircaloy-4.

were the lowest in a comparison with the other conditioned claddings. The pre-oxidized oxide layers (~6 μm) of the pre-oxidized claddings were thinner in comparison to the pre-hydrogenated/pre-oxidized claddings, and they were denser than the other ones because they were formed in the 450 °C steam condition. These relatively thinner and denser oxide layers could affect the oxidation rate at high temperatures above 900 °C. From this phenomenon, it is thought that the physical properties of the pre-formed oxide layer would strongly influence the oxidation kinetics and the oxidation rate at the LOCA temperatures.

In the case of the Zircaloy-4 claddings of Fig. 8(b), the oxidation rate constants of the samples having 80 μm OT with 600 wppm H were higher than those of the 30 μm OT with 250 wppm H. This could be due to the existing vertical cracks within the oxide layer formed during the sample preparation

process. If there were several vertical cracks within the oxide layer formed at the lower temperatures of less than 500 °C, they could affect the oxidation rate constants at temperatures above 900 °C during a steam oxidation. The existing cracks could play the role of an oxygen transportation during a steam oxidation at the LOCA temperatures. They would accelerate the oxidation rate when compared to an oxidation without vertical cracks. In Zircaloy-4, an oxidation retardation by the pre-formed layers was shown in the pre-hydrogenated/pre-oxidized claddings with 30 μm OT with 250 wppm H and the pre-oxidized ones. A thinner and denser, sound oxide layer would result in more retardation effects during a steam oxidation at temperatures above 900 °C.

3.4. Surface appearances and microstructures

After the oxidation tests at 900–1200 °C, the surface appearances were observed for the as-received claddings, as shown in Fig. 9. The surface colors were changed from a dark black to a gray color as the oxidation temperature increased. An oxidation temperature for the same duration of 2400 s would change the surface colors of the specimens. Similar trends were also revealed for the pre-oxidized and the pre-hydrogenated/pre-oxidized claddings. Fig. 10 shows the typical microstructures of the as-received claddings after the oxidation tests at 1100 °C. The microstructure of the as-received HANA-4 claddings was different from that of the Zircaloy-4. The thicknesses of the oxide layer and the oxygen-stabilized α-Zr layer of HANA-4 were thinner than those of Zircaloy-4. The thinner thicknesses of the layers in HANA-4 could be attributed to the lower oxidation rate constants. The border line between the oxygen-stabilized α-Zr layer and the prior β-Zr layer was clearly distinguished in Zircaloy-4. But the O-stabilized α-Zr layer in the HANA-4 cladding could not be clearly distinguished between the oxide and prior-β layers. The O-stabilized α-Zr phases could be incorporated into the prior β-Zr phases for the HANA-4 cladding. This could also be interpreted from the effects of a niobium addition to the HANA-4 cladding, from the results of Bohmert et al. [28]. The Sn segregation line [29–31] in the Zircaloy-4 oxide layers were easily detected in a temperature range above 1100 °C. But the line could not be detected in the oxide layers of the HANA-4 claddings. The absence of the Sn segregation line in the oxide layers of the HANA-4 claddings cannot be explained as yet. But the absence of the Sn line in the HANA-4 claddings could also be related to the alloying composition.

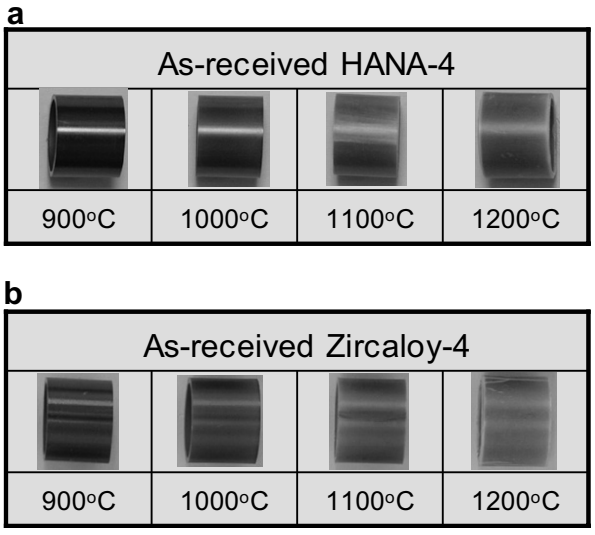

Fig. 9. Surface appearances after the oxidation tests at temperatures of 900–1200 °C: (a) as-received HANA-4, (b) as-received Zircaloy-4.

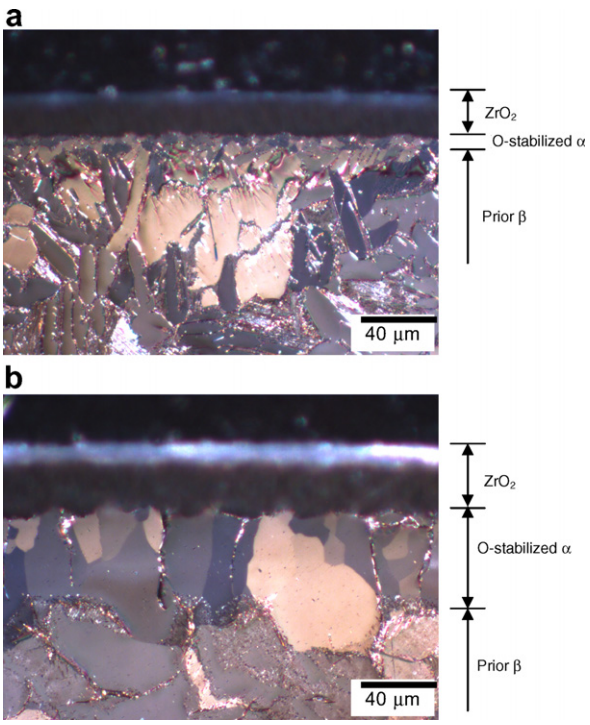

Fig. 10. Optical microstructures after the oxidation tests at 1100 °C: (a) as-received HANA-4, (b) as-received Zircaloy-4.

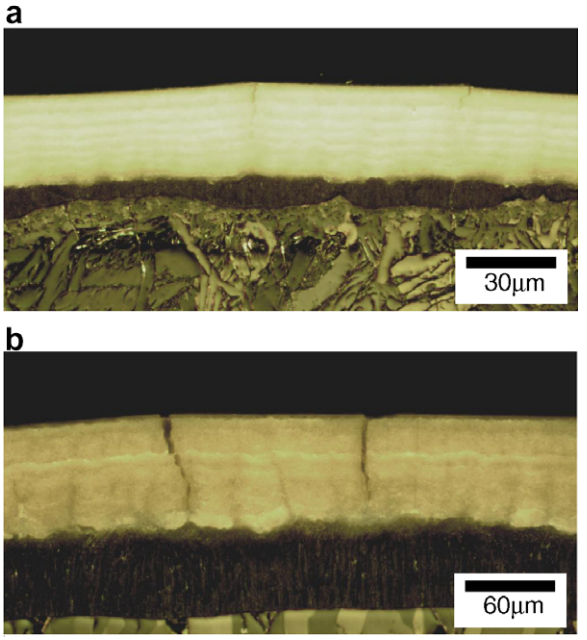

Fig. 11. Oxide layer morphologies of the pre-hydrogenated/pre-oxidized Zircaloy-4 at 1100 °C: (a) 30 μm OT with 250 wppm H, (b) 80 μm OT with 600 wppm H.

The microstructural properties of the pre-oxidized claddings were very similar to the as-received claddings. However, the pre-oxidized layer could reduce the oxidation rate at high temperatures above 900 °C. In the case of the pre-hydrogenated/pre-oxidized claddings, the microstructures were different from those of the as-received and the pre-oxidized claddings. A new oxide layer formed, during the steam oxidation, was appeared between the former pre-hydrogenated/pre-oxidized layer and the metal matrix when oxidized at 900–1200 °C under a steam atmosphere, as shown in Fig. 11(a). The new thick oxide layer, in Fig. 11(b), could be occasionally observed beneath some vertical cracks. This means that the vertical cracks could accelerate the steam oxidation rate at LOCA temperatures above 900 °C.

In short, the oxide layer formed under a normal operation could affect the steam oxidation rate at the LOCA temperatures. From the present study, there would be a critical thickness of the oxide layer to influence the steam oxidation rate. Since a sound oxide layer without vertical cracks would reduce the high-temperature oxidation rate, an improvement of the in-reactor corrosion resistance during a normal operation in a PWR is very important to maintain the LOCA stability of the fuel rods.

4. Conclusions

The steam oxidation resistance of HANA-4 was superior to that of Zircaloy-4 at the LOCA temperatures of 900–1200 °C, regardless of the pre-oxidization. This result could have resulted from a difference in the alloying composition between HANA-4 and Zircaloy-4. That is, the Nb as well as Sn within the HANA-4 cladding could have attributed to the improvement of the oxidation resistance in the high-temperature range. The higher Nb and the lower Sn in the HANA-4 cladding could change the microstructures during a steam oxidation. The microstructures of the HANA-4 cladding were represented as a thinner oxygen-stabilized α-Zr layer as well as incorporating α-Zr within the prior β-Zr layer, when compared to those of Zircaloy-4. The microstructural difference between the HANA-4 and Zircaloy-4 claddings could affect the oxidation behaviors and the rate constants of a high-temperature oxidation at 900–1200 °C. When the pre-oxidized layer on the cladding surface was formed at lower temperatures below 500 °C, a steam oxidation at high temperatures above 900 °C could be retarded significantly. And the vertical cracks within the pre-formed oxide layer decreased the effects of the oxidation rate's retardation. The soundness of the pre-oxidized layer formed at a lower temperature could influence the oxidation kinetics and the rate constant during a steam oxidation at the LOCA temperatures of 900–1200 °C.

Acknowledgments

This study was supported by Korea Science and Engineering Foundation (KOSEF) and Ministry of Science and Technology (MOST), Korean Government, through its National Nuclear Technology Program.

References

[1] K.S. Lee, Introduction to Nuclear Fuels, Korea, 2001.
[2] USNRC-SRP (Standard Review Plan), Sec. 4.2, NUREG-0800.
[3] G.P. Sabol, R.J. Comstock, R.A. Weiner, P. Larouere, R.N. Stanutz, Zirconium in the Nuclear Industry, ASTM STP 1245, 1994, p. 724.
[4] J.-P. Mardon, D. Charquet, J. Senevat, Zirconium in the Nuclear Industry, ASTM STP 1354, 2000, p. 505.
[5] T. Isobe, Y. Matsuo, Zirconium in the Nuclear Industry, ASTM STP 1132, 1991, p. 346.
[6] T. Harada, M. Kimpara, K. Abe, Zirconium in the Nuclear Industry, ASTM STP 1132, 1991, p. 368.

[7] Y. Etoh, S. Shimada, T. Yasuda, T. Ikeda, R.B. Adamson, J.-S. Fred Chen, Y. Ishii, K. Takai, Zirconium in the Nuclear Industry, ASTM STP 1129, 1996, p. 825.
[8] Y.H. Jeong, S.Y. Park, M.H. Lee, B.K. Choi, J.G. Bang, J.H. Baek, J.Y. Park, J.H. Kim, H.G. Kim, Y.H. Jung, in: Proceedings on the 2005 Water Reactor Fuel Performance Meeting, Kyoto, Japan, 2005.
[9] Y.H. Jeong, J.H. Baek, J.Y. Park, in: Proceedings of IAEA Technical Meeting on Corrosion Resistance Zirconium Alloys, Buenos Aires, Argentina, 2005.
[10] F.J. Erbacher, S. Leistikow, Zirconium in the Nuclear Industry, ASTM STP 939, 1987, p. 451.
[11] F.C. Iglesias, S. Sagat, H.E. Sills, Res. Mech. 17 (1986) 125.
[12] J.-C. Brachet, J. Pelchat, D. Hamon, R. Maury, P. Jacques, J.-P. Mardon, in: TCM on Fuel Behavior Under Transient and LOCA Conditions Organized by IAEA, Halden, Norway, 10–14 September 2001.
[13] R.E. Pawel, J.J. Campbell, ASTM STP 754, 1982, p. 370.
[14] V.F. Urbanic, ASTM STP-633, 1977, p. 168.
[15] H.M. Chung, G.R. Thomas, ASTM STP-824, 1984, p. 793.
[16] A. Swatzky, G.A. Ledoux, S. Jones, ASTM STP-633, 1977, p. 134.
[17] M. Aomi, N. Nakatsuka, S. Komura, T. Hirose, T. Anegawa, in: Proceedings on ANS Topical Meeting, City Park, USA, 2000.
[18] J.V. Cathcart, R.E. Pawel, R.A. McKee, R.E. Druschel, G.J. Yurek, J.J. Campbell, S.H. Jury, ORNL, ORNL/NUREG-17, 1977.
[19] J.-P. Mardon, A. Lesbros, C. Bernaudat, N. Waeckel, in: Proceedings of the 2004 International Meeting on LWR Fuel Performance, Orlando, USA, 2004, p. 507.
[20] J.H. Baek, K.B. Park, Y.H. Jeong, J. Nucl. Mater. 335 (2004) 443.
[21] S. Kawasaki, T. Furuta, M. Suzuki, J. Nucl. Sci. Technol. 15 (8) (1978) 589.
[22] H. Uetsuka, T. Otomo, J. Nucl. Sci. Technol. 26 (2) (1989) 240.
[23] L. Baker, L.C. Just, ANL-6548, 1962.
[24] R.E. Pawel, J.V. Cathcart, R.A. McKee, J. Electrochem. Soc., Electrochem. Sci. Technol. 126 (7) (1979) 1105.
[25] H. Uetsuka, F. Nagase, in: Proceedings on ANS Topical Meeting, City Park, USA, 2000.
[26] M. Ozawa, T. Takahashi, T. Homma, K. Goto, Zirconium in the Nuclear Industry, ASTM STP 1354, 2000, p. 279.
[27] H. Ocken, R.R. Biederman, C.R. Hann, R.E. Westerman, Zirconium in the Nuclear Industry, ASTM STP 681, 1979, p. 514.
[28] J. Bohmert, M. Dietrich, J. Linek, Nucl. Eng. Des. 147 (1993) 53.
[29] J.T. Prater, E.L. Courtright, Zirconium in the Nuclear Industry, ASTM STP 939, 1987, p. 489.
[30] R.E. Pawel, R.A. Perkins, R.A. Mckee, J.V. Cathcart, G.J. Yurek, R.E. Druschel, Zirconium in the Nuclear Industry, ASTM STP 633, 1977, p. 199.
[31] W.G. Dobson, R.R. Biederman, R.G. Ballinger, Zirconium in the Nuclear Industry, ASTM STP 633, 1977, p. 150.